IEEE Transactions on Nuclear Science, Vol. NS-30, No. 4, August 1983

A TRANSVERSE-FIELD-FOCUSSING (TFF) ACCELERATOR FOR INTENSE RIBBON BEAMS

O. A. Anderson, D. A. Goldberg, W. S. Cooper, and L. Soroka
Lawrence Berkeley Laboratory
University of California
Berkeley, CA 94720

Abstract

In a TFF Accelerator, a transverse electric field is set up between pairs of curved deflecting plates. Charged particles passing between the plates are both deflected and strongly focussed by the field. Average-straight-line motion (if desired) is obtainable by having the successive pairs of plates curve in alternating directions (with corresponding reversal of the field). Acceleration is achieved by adjusting the mean voltage on each succeeding pair of plates. Computer simulations are in good agreement with the analytically calculated beam dynamics; they show no evidence of beam instabilities and almost no emittance growth. A design for a 400 keV, 8 A/meter, single-ribbon dc accelerator will be presented.

1. Introduction

Transverse field focussing of ribbon beams is a well-known effect[1,2] which has been used in electron beam transport[3] and electrostatic analyzers.[4] We discuss here a new application, the transport and acceleration of high power ion beams (10 A dc, 400 to 800 keV) needed in neutral injection systems for fusion reactors. Transverse field focussing (TFF) has been shown to be capable of meeting all the requirements of such a beam system.[5-7] Analytic calculations have shown that the current densities and emittances transportable in a TFF device exceed those obtainable with electrostatic quadrupoles using comparable potentials and gradients.[5]

This paper summarizes the basic formulae that we have derived to describe TFF physics, and presents a typical accelerator design. (A more detailed account will be published separately.)[8] We analyze some topics not previously treated for ribbon beams, such as effects of electrode gaps and beam emittance, and the condition for beam matching.

In Section 2 we discuss the equilibrium trajectory, Poisson's equation, single-particle oscillations, the envelope equation, and the matched beam condition. Section 3 summarizes the analysis of electrode gap effects for application to beam matching. Formulae for optimizing a beam transport system are derived in Section 4, and acceleration is discussed in Section 5. We conclude, in Section 6, by applying all these results to the design of a proposed 400 keV accelerator.

Other topics, such as design of matching sections and control of the beam edge, will be discussed elsewhere.[8]

2. Basic Equations for Transport

We are considering negative ions with energies < 1 MeV and use non-relativistic equations. (Our equations, with slight alterations, also apply to positive ions.) We assume that negative ion beams have had any accompanying electrons removed prior to acceleration. We note that low energy electrons created by collisions with gas in the accelerator will be immediately swept out by the TFF fields.

First, we analyze ribbon beam dynamics in the regions between the curved electrodes (Fig. 1); we include gap effects later. We consider concentric cylindrical-arc electrodes and a concentric ion trajectory at the mean radius r_m. If we assume this ion was born somewhere at zero potential we have $mv^2/2 = -q\phi_m$ where ϕ_m is the potential at r_m that results from the electrode potentials and the space charge of the total beam. Then force balance requires a radial electric field at r_m

$$E_m = \frac{2\phi_m}{r_m}, \tag{1}$$

an expression which will be used frequently.

Our model is a ribbon beam with thickness $2x_0$ centered about r_m and carrying a uniform current density $J = I_1/2x_0$, where I_1 is the current per unit width. Integrating Poisson's equation in cylindrical coordinates using E_m from Eq. (1) as an initial condition gives[8]

$$\frac{\phi}{\phi_m} = 1 - 2\ln(1+\frac{x}{r_m}) + 2k\frac{x^2}{r_m^2} + O(\frac{x^4}{r_m^4}) \tag{2}$$

for $x=r-r_m$, $-x_0<x<x_0$. (Terms through 5th order and electrode potentials are calculated in Ref. 8. In the present paper we keep ϕ terms only through x^2.) We have introduced $k=k'/x_0$ where

$$k' = Cr_m^2 I_1/\phi_m^{3/2} \tag{3}$$

with $C = \pi/2(2e/m)^{1/2}$. ($C = 1.45\times10^6$ for D⁻ beams or 2.05×10^6 for H⁻ beams when I_1 is in A/cm and ϕ is in volts.) Perturbing an equilibrium orbit in the potential given by Eq. (2), we obtain the single-particle equation

$$\frac{d^2x}{ds^2} + \frac{2}{r_m^2}(1-k)x = 0 , \tag{4}$$

where s is the distance along the midline.

Our transport system (Fig. 1) consists of a series of electrodes with alternating curvature separated by short gaps and arranged to give a constant potential along the midline of the beam (equilibrium orbit). The envelope x_0 can no longer be exactly constant, because of the gaps. Equation (4) still applies in the modified form[8]

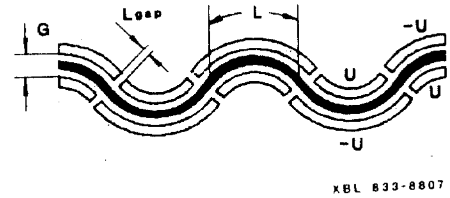

Fig. 1. TFF transport system, with notation used in this paper.

$$\frac{d^2x}{ds^2} + \frac{2}{r_m^2}\left(f(s) - \frac{k'}{x_0}\right)x = 0\ , \qquad (5)$$

where $f(s) = E^2(s)/E_m^{\ 2}$ with $E(s)$ the field along the midline. Then $f > 0$ in the gaps, and $f = 1$ in the electrode sections; f is periodic with period L, where L is the distance between gaps. If

$$x_0(s+L) = x_0(s) \qquad (6)$$

the beam is called matched and has small Floquet oscillations; otherwise there are envelope oscillations with a different period. We do not discuss the latter here, except to note they may be used for beam matching purposes.[8] Imposing (6) and using Floquet's theorem and standard methods developed for AG systems,[9] we obtain

$$\frac{d^2x_0}{ds^2} + \frac{2}{r_m^2}\left(f(s)\,x_0 - k'\right) - \frac{\varepsilon^2}{x_0^3} = 0\ , \qquad (7)$$

where ε is the (unnormalized) emittance. (This equation can also be derived from a different point of view, starting with the Vlasov equations.[8])

Since $f(s)$ is non-negative in TFF (rather than alternating in sign) and the gaps are short, the Floquet oscillations described by Eq. (7) are considerably smaller than in AG systems. Averaging Eq. (7) over the period L yields the important result (accurate to within 0.5%) for a matched beam[8]

$$k + \eta^2 = f\ , \qquad (8)$$

where $k = k'/\langle x_0\rangle$,

$$\eta^2 = \frac{r_m^2}{2}\,\frac{\varepsilon^2}{\langle x_0\rangle^4}\ , \qquad (9)$$

and $f = \langle f(s)\rangle$, a constant determined by the geometry. Equation 8 shows how the matched beam condition (6) can be satisfied by various ratios of the space charge term to the emittance term. Equation (8) was derived for a transport system but can be applied with due care to accelerators where most parameters, including L, change slightly from one electrode pair to the next (see Section 6).

3. Electrode Gap Effect

In order to calculate f for a TFF transport section, we applied conformal mapping techniques to an idealized electrode geometry[10] in order to obtain the transverse electric field $E(s)$ along the midline, and then computed $\langle 1-E^2(s)/E_m^{\ 2}\rangle$. The result The result is shown as a function of gap length in Fig. 2. This result applies to all cases where the electrodes are long enough for $E(s)$ to essentially reach the maximum possible value E_m, i.e., for $L/G > 3$ (see Fig. 1). In practice L_{gap}/G is in the range between 0.35 and 1.45, and then f is well-represented by the linear approximation

$$f = 1 - 0.65\,\frac{L_{gap}}{L} - 0.45\,\frac{G}{L}\ . \qquad (10)$$

In a TFF accelerator there is a conventional accelerating-gap field superposed on the transport field, and its focussing effect increases f by up to 10%.[8,10]

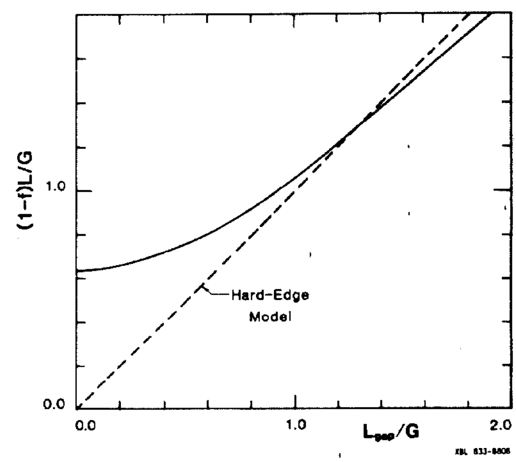

Fig. 2. Result of electrode gap calculation.

4. Maximizing Current Transport

Consider a matched beam with given emittance and energy. Equations (3) and (8) show that I_1 can be increased by suitably varying x_0 or r_m, but the electric fields or potentials calculated using Eq. (1) could become unacceptably large. A potential limit usually turns out to be the controlling factor, so we will maximize I_1 with fixed U, where U is the potential of an electrode with respect to the beam. We define a safety factor $S = G/2x_0$ which allows clearance needed for any beam envelope oscillations or for a halo from aberrations in the injected beam. We have $\langle x_0\rangle = ar_m$ where $a = U/4S\phi_m$ is constant. (We used Eq. (1) and the approximation $U = E_mG = 2E_mr_0S$.) Thus we can write Eq. (8) as

$$\frac{CI_1}{\phi_m^{3/2}}\,\frac{r_m}{a} + \frac{\varepsilon^2}{2r_m^2a^4} = f\!\left(\frac{L_{gap}}{L},\ a,\ \frac{r_m}{L}\right)\ , \qquad (11)$$

where f is expressed in a general way which allows for inclusion of focussing by an acceleration field. If we maintain constant shape, i.e., scale L and L_{gap} with r_m, then f is constant and we find by differentiation of (11) that

$$r_{opt} = \left(\frac{3}{2f}\right)^{1/2}\frac{\varepsilon}{a^2}$$

so that

$$I_1^{max} = \frac{\phi_m^{3/2}}{C}\left(\frac{2f}{3}\right)^{3/2}\frac{a^3}{\varepsilon} \qquad (12)$$

for the case considered. We can express the results in the form

$$k = \frac{2}{3}f\ , \qquad (13)$$

which is useful for making quick estimates, since f is typically 0.8 and k is $9J/J_{CL}$ where J_{CL} is the Child-Langmuir current density in a plane diode with spacing r_m. Physically, Eq. (13) says that for a matched beam in a system optimized in the manner discussed, the space charge force should be twice the emittance effect (thermal pressure gradient[8]) and the sum of these forces equals the average focussing force.

Many other optimizations are possible; for example, L may be held fixed instead of scaling with r_m, in which case Eq. (12) and (13) will have correction terms.[8]

5. Acceleration

Our equations so far were developed for a periodic system, but it is reasonable to apply them to an accelerator if the fractional change in beam energy per gap is sufficiently small. At this point we introduce the (constant) normalized emittance $\epsilon_n = v\epsilon/c$ so that the matched beam condition, Eq. (8), is

$$\frac{CI_1}{X}\frac{r^2}{\phi^{3/2}} + \frac{\epsilon_n\ mc^2}{4eX^4}\frac{r^2}{\phi} = f\ , \tag{14}$$

where for simplicity we put $\phi_m=\phi$, $r_m=r$, and $\langle x_0\rangle=X$. We choose to keep X constant from one section to another (an option). We introduce subscript F for the reference section optimized for maximum I_1 at fixed U. (This turns out to be the final section.) Then by Eq. (13)

$$\frac{CI_1}{X}\frac{r_F^{\ 2}}{\phi_F^{\ 3/2}} = \frac{2}{3}f_F\ ,$$

so that the other term in Eq. (14) is $f_F/3$. Substituting in (14) and rearranging, we find

$$\frac{r}{r_F} = \left(\frac{\phi}{\phi_F}\right)^{3/4} g^{1/2}\ , \tag{15}$$

where $g = \dfrac{3f/f_F}{2 + (\phi/\phi_F)^{1/2}}$ is a correction factor near unity. We also find that

$$\frac{U}{U_F} = \left(\frac{\phi}{\phi_F}\right)^{1/4} g^{-1/2}\ , \tag{16}$$

which shows that the transverse electrode potential difference is greatest at the exit of the accelerator.

6. Design of a 400 keV Accelerator

Figure 3 shows the configuration of a proposed 400 keV, 8A/meter H^- accelerator which we designed using the above equations. The figure also shows the numerically computed self-consistent beam trajectories, which are in excellent agreement with prediction. (Details on phase space dynamics will be published elsewhere.[8]) We started with the specifications U_{max}=50kV, S=3, and ϵ=0.025 πrad-cm at the injection energy of 80 keV. The gap field limit was 40 kV/cm. (The maximum transverse field turned out to be 23 kV/cm.) We chose a 6 gap accelerator giving 30% energy gain per stage, and imposed reasonable limits on the lengths L. These considerations determined that r_F be 34 cm for the final stage, and that I_1 be 8A/meter of H^-.

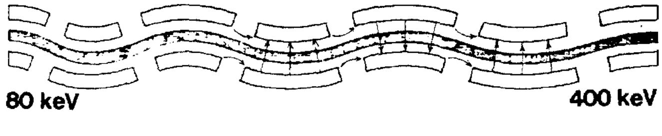

Fig. 3. Computation for TFF 400 keV, 8A/m H^- accelerator. Total length is 92 cm. Arrows are in direction of electric force.

Acknowledgments

The authors greatly appreciate the contributions of Klaus Halbach in the analysis of electrode potentials, and the encouragement of R. V. Pyle and W. B. Kunkel.

This work was supported by the Director, Office of Energy Research, Office of Fusion Energy, Development and Technology Division of the U. S. Department of Energy under Contract NO. DE-AC03-76SF00098.

References

1. J. R. Pierce, Theory and Design of Electron Beams, 2nd ed. (D. Van Nostrand, New York, 1954).

2. P. T. Kirstein, G. S. Kino, W. E. Waters, Space Charge Flow, (McGraw-Hill, New York, 1967).

3. H. A. C. Hogg, "Periodic Electrostatic Beam Focussing," Proc. IEE, Part B, Suppl. 12-13, p. 1016 (1958).

4. P. Dahl. Introduction to Electron and Ion Optics, (Academic Press, New York, 1973).

5. O. A. Anderson, "The TFF Accelerator for Fusion Reactor Injection;" see also four other TFF-related papers in Bull. Am. Phys. Soc., 27 (8), part II, pp. 1141-1142 (1982).

6. O. A. Anderson, W. S. Cooper, D. A. Goldberg, L. Ruby, L. Soroka, "Negative-Ion-Based Neutral Beam System for FED-A Current Drive," LBL-14880, August 1982, to be published in Considerations of an Advanced Performance Fusion Engineering Device (FED-A), Oak Ridge National Laboratory Report ORNL/TM 8498, 1982.

7. O. A. Anderson, W. S. Cooper, D. A. Goldberg, L. Ruby, L. Soroka, J. H. Fink, "Efficient Radiation-Hardened 400 and 800 keV Neutral Beam Injection Systems," to be published in Proceedings of the 5th Topical Meeting on the Technology of Fusion Energy, Knoxville, TN, April 26-28, 1983.

8. O. A. Anderson, in preparation.

9. H. C. Corben, P. Stehle, Classical Mechanics, 2nd ed. (R.E. Krieger, New York, 1974).

10. D. A. Goldberg and K. Halbach, to be published.